

B-WIM systems application on reinforced concrete bridge structural assessment and highway traffic characterization

Aplicação de sistemas B-WIM para avaliação estrutural e caracterização do tráfego em uma ponte de concreto armado

P. JUNGES^a
paulojunges@gmail.com

R. C. A. PINTO^b
r.pinto@ufsc.br

L. F. FADEL MIGUEL^b
leandro.miguel@ufsc.br

Abstract

The vehicles that travel on Brazilian highways have changed a lot in the last decades, with an increase in the traffic load and in the amount of trucks. This fact is not exclusive to our country, so much that in order to assess the structural safety of bridges, there was a great development in bridge weigh-in-motion systems (B-WIM) the last decade, especially in developed countries. Moses, in 1979, was the first one to introduce the B-WIM concept. This work presents the results of a B-WIM system applied on a bridge over the Lambari river, located at BR 153 in Uruaçu (Goiás). The weigh-in-motion technique used is based on Moses' Algorithm and uses influence lines obtained direct from traffic. Traffic characterization of that particular highway, as well as the effects introduced in the bridge structure and the experimental dynamic amplification factor are also discussed. At the end it is concluded that the system used is capable of detecting, with good precision, the axle spacing and the gross vehicle weight shows errors inferior to 3% when compared with the gross weight acquired with static scale.

Keywords: B-WIM, monitoring, traffic characteristics, bridges, safety.

Resumo

Os veículos que trafegam nas rodovias brasileiras mudaram muito nas últimas décadas, ocorrendo um aumento na capacidade de carga e na quantidade de caminhões. Esse fato não é exclusivo do nosso país, tanto que na última década houve um grande desenvolvimento dos sistemas de pesagem em movimento em pontes (bridge weigh-in-motion, B-WIM), especialmente nos países desenvolvidos, para avaliação da segurança estrutural de pontes. Moses em 1979 foi o primeiro a introduzir o conceito de B-WIM e o algoritmo por ele desenvolvido continua sendo o mais popular nos sistemas comerciais. No presente estudo são mostrados os resultados da utilização de um sistema B-WIM no monitoramento de uma ponte sobre o rio Lambari, na BR 153, no município de Uruaçu (Goiás). A técnica de pesagem em movimento empregada é baseada no algoritmo de Moses e utiliza linhas de influência obtidas diretamente do tráfego. A caracterização do tráfego atuante nessa rodovia, bem como os esforços introduzidos na estrutura da ponte e um coeficiente de impacto obtido de forma experimental são também discutidos. Ao final conclui-se que o sistema empregado é capaz de detectar com boa precisão o espaçamento entre os eixos e o peso bruto total dos veículos apresenta erros inferiores a 3% quando comparados com os pesos obtidos em balança estática.

Palavras-chave: B-WIM, monitoramento, característica do tráfego, pontes, segurança.

^a Civil Engineering Department, Federal University of Mato Grosso;

^b Programa de Pós Graduação em Engenharia Civil, Universidade Federal de Santa Catarina, Florianópolis, Santa Catarina, Brasil.

1. Introduction

The live load model used in Brazil has not changed much in the last forty years. Since the NB-6 from 1960 [1], the live load in bridges consists of a standard vehicle with six wheels distributed on three equally spaced axles of 1.5 m. On the other hand, the vehicles that travel on the Brazilian Highways have changed a lot in the last decades, with an increase in the load capacity and in the amount of trucks. Moreover, new classes of vehicles emerged, being common nowadays the presence of trucks up to nine axles and 30 meters long.

Therefore, the load from the traffic should be better assessed to ensure bridge safety. According to [2], these changes in the traffic need to be regularly taken into account by means of code calibration. B-WIM systems, which allow the effective estimation of traffic over the bridge, have had a great development in recent years [3], both in terms of safety assessment of existing structures and on the determination of design loads.

The B-WIM concept was introduced by Moses [4] in the late 70s. An algorithm with his name uses the influence line (IL) concept in order to acquire the weight of the vehicles that travel over bridges with girders. In the 80s, Peters ([5] and [6]) developed weigh-in-motion systems for use on bridges (AXWAY) and culverts (CULWAY), having reached good results for gross vehicle weight estimation (GVW), but inaccurate results for weight of close axles.

In the 90s, two B-WIM systems emerged at the same time in Slovenia and Ireland [7], both result of the COST 323 [8] and WAVE [9] projects. The DuWIM system was developed by researchers of Trinity College Dublin and University College Dublin. It uses point-to-point manual graphical method to acquire the bridge IL from the passage of a calibration vehicle over the bridge. The SiWIM system, developed by the Slovenian Institute of Civil Engineering and Construction (ZAG) team, uses an optimization algorithm after the vehicle weight was determined by Moses' algorithm in order to improve the results. In addition, the SiWIM system does not use axle

detection sensors over the bridge. Both DuWIM and SiWIM were also developed to orthotropic bridges applications.

In the 2000s, Yamada and Ojio [10] developed a B-WIM system in which the support stiffeners of a steel bridge are instrumented to measure the vertical strains. However, the method is not very accurate since, according to the authors, only one element is the instrumented.

In all these aforementioned methods, the axles weight identification is nothing more than an optimization problem [11]. In this sense, authors like Jiang et al [12], Au et al [13], Law et al [14], Deng and Cai [15], Pan and Yu [16] and Kim et al [17] sought to employ different optimization techniques to solve the problem, from the use of genetic algorithms to artificial neural networks.

Besides these systems in time domain, several authors proposed methods that use the bridge dynamic response ([18], [19], [20], [21] e [22]). Nevertheless, these methods are still quite complex and difficult to implement.

In 2005, Karoumi, Wiberg and Liljencrantz [23] extended the B-WIM utilization to railway bridge monitoring. The developed system uses strain transducers placed at different points in order to detect the axles and to calculate the velocity. In Brazil, Carvalho Neto e Veloso [24] developed a similar system to characterize the railroad traffic.

Despite all the progress, Moses' algorithm continues to be the ideal choice in the implementation of B-WIM systems due its simplicity and good precision, provided that certain requirements are met [11]. In this way, in order to assess the efficiency of this system on the bridges of the Brazilian road network, a bridge at BR 153 highway has been monitored during 42 days. From this monitoring, information was obtained about the traffic and structure behavior in terms of IL and internal forces distribution.

2. Bridge weigh-in-motion systems (B-WIM)

Broadly used in developed countries for bridge structural safety assessment, B-WIM techniques are already applied in some of these

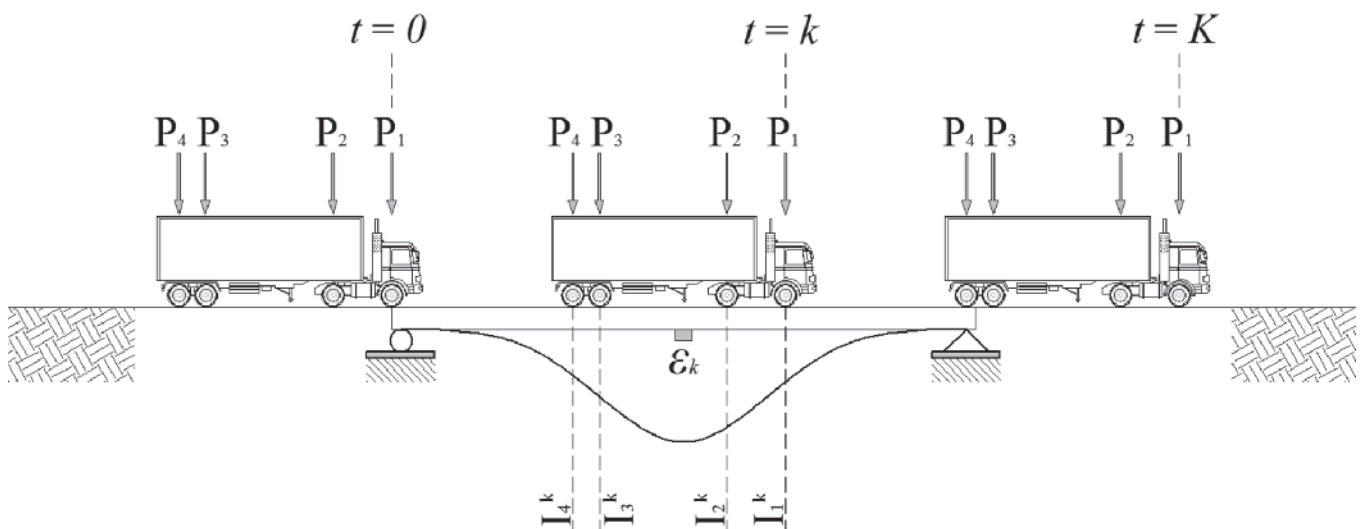


Figure 1
Influence line for bending moment for a 4-axle vehicle

countries to determine the design live load for bridges. According to Žnidarič e Žnidarič [25], on B-WIM application, the vehicle stay in contact with the bridge for a long time period, which makes possible to acquire a large amount of measurements and therefore, smooth the dynamic effects. Besides, the main advantage of a B-WIM system is that it is portable and does not interfere with the traffic during its installation [2].

B-WIM concepts were first introduced by Moses [4] in 1979, using the principle that a live load along the bridge introduce stresses proportional to the product of the IL ordinate with the load magnitude. The weight of the trucks that travel over a bridge is obtained by a function that minimizes the error between the measured stresses and the theoretical ones.

Thus, a truck traveling with a constant velocity produces a response that varies over time in equally intervals (k). Observing Figure 1 and considering the superposition principle, the theoretical maximum bending moment, in a k instant, is given by Equation (1).

$$M_{ST}^k = \sum_{i=1}^N P_i I_i^k \tag{1}$$

where M_{ST}^k = theoretical bending moment; N = number of vehicle axles; P_i = weight of the i^{th} vehicle axle; I_i^k = IL ordinate for the i^{th} axle for k scan.

Moses has used the fact that the stress in each girder is related with bending moment by the relationship indicated in Equation (2) and has acquired the active bending moment in the bridge, in an instant k , as defined by Equation (3), considering that all girders have the same properties.

$$M_j = W_j \sigma_j = EW_j \varepsilon_j \tag{2}$$

$$M_{SE}^k = EW \sum_{j=1}^m \varepsilon_j^k \tag{3}$$

where E = modulus of elasticity of the bridge material; W_j = elastic section module for the j^{th} girder; M_{SE}^k = experimental bending moment in a time instant; m = number of girders; ε_j^k = strain of the j^{th} girder in a time instant.

Dynamic effects of the truck-pavement-structure system are included in the value of the experimental bending moment. As the measured response is acquired during the whole passage of the vehicle over the bridge, these dynamic effects can be smoothed out by an error function that minimizes the sum of the squares differences between the experimental and theoretical bending moments, as shown in Equation (4). This minimization process allows to obtain loads closer to the real static values.

$$\varphi = \sum_{k=1}^K (M_{SE}^k - M_{ST}^k)^2 \tag{4}$$

where φ = error function; k = scan number; K = total number of scans.

The minimization process of Equation (4) in relation to the j^{th} axes results in Equation (5). This equation can be rewritten in a matrix form, as defined by Equation (6), as a function of the influence lines matrix $[F]$ and the vector that relates the measured bending moments and the IL ordinates $\{M\}$.

$$\sum_{k=1}^T \left[\sum_{i=1}^n P_i I_i^k \right] I_j^k = \sum_{k=1}^T M_{SE}^k I_j^k \tag{5}$$

$$\{P\} = [F]^{-1} \{M\} \tag{6}$$

$$[F] = \sum_{k=1}^T I_i^k I_j^k \tag{7}$$

$$\{M\} = \sum_{k=1}^T M_{SE}^k I_j^k \tag{8}$$

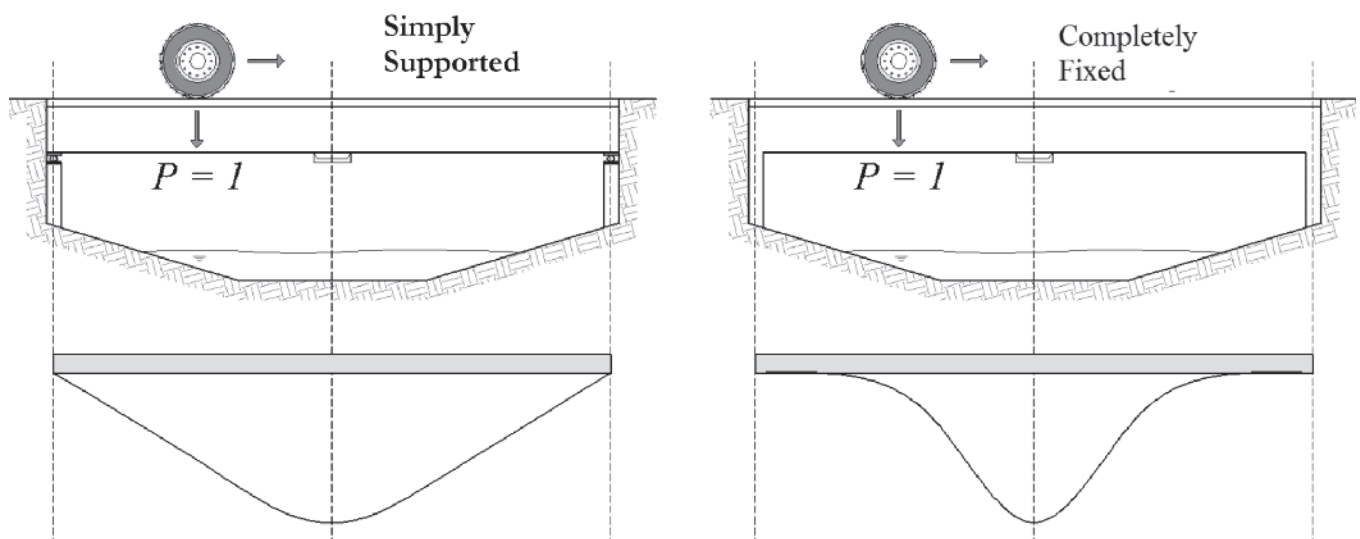


Figure 2 Influence line for bending moments at midspan of bridges simply supported and completely fixed

where T = total number of time intervals used; $\{P\}$ = vector of axles weight; $[I]$ = influence lines matrix for bending moment; $\{M\}$ vector that relates the measured bending moments and the IL ordinates. Each element of vector $\{P\}$, defined by Equation (6), represents the weight of one of the axles of the vehicle. The GVW is given by the sum of the elements of this vector.

The efficiency of Moses' algorithm here presented is affected mainly by the dynamic effect of vehicles in movement, by the transverse position of the vehicles and the final equation system [11]. The dynamic effect of vehicles is directly related to the pavement roughness and bridge entrance conditions. The greater the dynamic effects, the lower will be the accuracy of the system, because greater will be the difference between measured and predict response using the static IL. Moreover, the algorithm does not take into account the number of lanes and hence does not account for the transverse load distribution, which could lead to significant errors. Finally, the final equation system can be ill conditioned in cases where noise in the measured signal is significant.

2.1 Calibração do sistema

In his study, Moses has used a theoretical IL in order to acquire trucks weights. However, according to Žnidarič and Baumgartner [26], the actual IL of the structure differs from the theoretical one; it is between the idealized conditions of simple supported and completely fixed support (Figure 2). Several authors have demonstrated the importance of using an IL that better describes the real structural conditions, as Žnidarič and Baumgartner [26], McNulty [27], González and O'Brien [28], McNulty and OBrien [29], Quilligan [30], Obrien, Quilligan and Karoumi [31], Junges, Pinto and Fadel Miguel [32], Ieng [33], Heinen, Pinto and Junges [34]. According to Obrien, Quilligan and Karoumi [31], although the IL can be easily obtained from the theoretical or numerical analysis of the structure, the results usually do not meet the ones measured on the bridge, being interesting to acquire the IL directly from the measured stresses coming from the passage of a vehicle with known weight. These authors have developed a mathematical method to calculate the IL directly from monitoring data. In the proposed method, there is no need to know the exactly position in which the applied load starts the bending of the bridge. Thus, uncertainty around the real support conditions and the small strain usually induced near the supports are avoided.

Using a vehicle with known axle weights, this method consists to minimize Equation (4) in respect to the R^{th} IL ordinate, resulting in the Equation (9) which can be rewritten in matrix form as shown in Equation (10).

$$\sum_{k=1}^T \left[\sum_{i=1}^n P_i I_i^k \right] P_j = \sum_{k=1}^T M_{SE}^k P_j \tag{9}$$

$$[W]\{I\} = \{MP\} \tag{10}$$

where $[W]$ = sparse and symmetric matrix dependent of axle weights; $\{I\}$ = vector containing the IL ordinates; $\{MP\}$ vector dependent of measured bending moments and axle weights. The IL ordinates are obtained by according to Equation (11).

$$\{I\} = [W]^{-1}\{MP\} \tag{11}$$

This procedure was validated on two reinforced concrete bridges located in Sweden [31], reaching excellent correlation between the measured response and the predicted one with the acquired IL. Nevertheless, this method may require a high computational cost, since it is necessary to invert a matrix that, for a three-axle truck and acquisition frequency of 1024 Hz, may be in the order of 1500 and 2000.

The B-WIM system used in the present study, developed initially by Žnidarič, Žnidarič e Terčelj [35], uses ILs obtained by means of the procedure proposed by [31] from the passage of trucks with known weights over the bridge. The IL calibration follows the indication of the COST 323 [8] report and the recommendations about weigh-in-motion published by ISWIM [36] to ensure a good quality in the results.

Based on the COST 323 [8] report, the calibration process of B-WIM systems, i.e., obtaining the actual bridge IL, consists of passing vehicles with known weights over the system several times. The greater the number of passages, the greater the accuracy of the system. These passages should be done with at least two vehicle classes (rigid and semi-trailer) at two velocity levels.

2.2 Axle detection sensors

In order to obtain velocity information, axle spacing and vehicle class that travel in the highway, strain transducers, called free-of-axle detector (FAD) sensors, are placed on the bottom of the bridge superstructure instrumented with B-WIM systems [37]. The FAD sensors are installed at a certain distance along the bridge length so that it is possible to acquire similar signals spaced by a time interval, as can be seen in Figure 3 for the passage of a 5-axle truck. From these signals, the vehicle velocity is calculated by an optimization process that results on the time interval which minimizes the difference between sensors readings [7], as defined by Equation (12).

$$\xi(\Delta t) = \sum_{t=1}^{TT} [\varepsilon_2(t + \Delta t) - \varepsilon_1(t)]^2 \tag{12}$$

where ξ = objective function; Δt = time for the truck to pass between two instrumented sections; TT = total time for the truck to

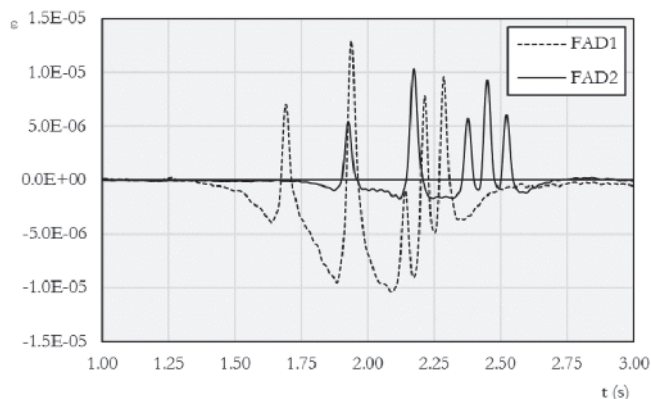


Figure 3 Signals obtained with FAD sensors for a 5-axle vehicle

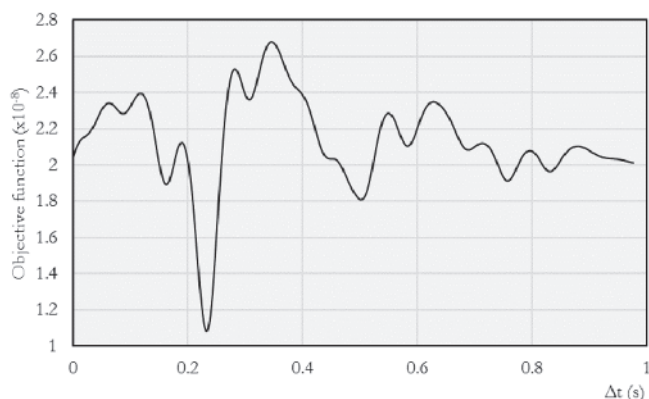


Figure 4
Acquiring the time interval which minimizes the objective function

pass the two instrumented sections; ϵ_1 , ϵ_2 = strain measured in section 1 e 2, respectively.

Figure 4 shows an example of the behavior of objective function (ξ) with time interval (Δt) varying between 0 and 1 s. From this figure, it is clear that a minimum global value for the time interval exists. Knowing the distance between sensors and using the time interval obtained by this optimization process, it is possible to acquire the vehicle velocity.

2.3 Dynamic amplification factor

The dynamic amplification factor, or impact coefficient, is calculated by the relationship between measured and static response, according to Equation (13).

$$DAF = \frac{\epsilon_{SE,max}}{\epsilon_{ST,max}} \quad (13)$$

where DAF = dynamic amplification factor; $\epsilon_{SE,max}$ = measured response; $\epsilon_{ST,max}$ = static response.

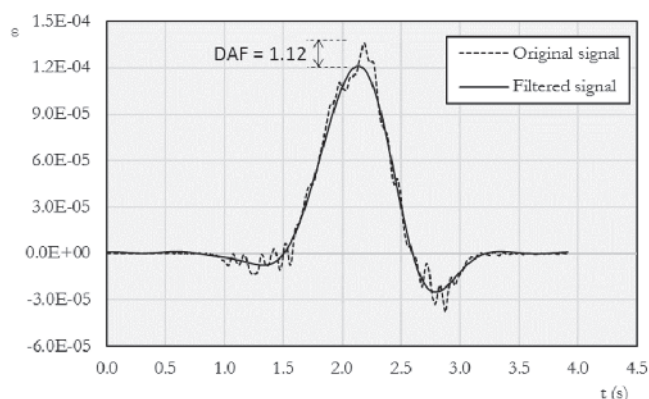


Figure 5
Bridge strain signal before and after the application of the gaussian filter

The static response can be obtained by the signal reconstruction, from the IL and axle weights, or by means of low-pass filters in the measured signal. The latter leading to better results (ARCHES D10 [38]).

Low-pass filters eliminate the response with frequency above certain threshold level. Therefore, the signal is smoothed, removing high frequency fluctuations and saving the low frequency ones. The moving average is the most usual low-pass filter, however the B-WIM system used in the present study uses a Gaussian filter.

The filtering process consists of making a convolution of the original signal and a Gaussian function, both in the frequency domain [39]. The Gaussian filter in one dimension is defined according to Equation (15).

$$g(x) = \frac{1}{\sqrt{2\pi}\sigma} \times e^{-\frac{x^2}{2\sigma^2}} \quad (14)$$

where $g(x)$ = Gaussian function; σ = standard deviation.

One of the best justifications for the good performance of the Gaussian filter is related with its response in the frequency domain. The Gaussian function defined in Equation (15) continues

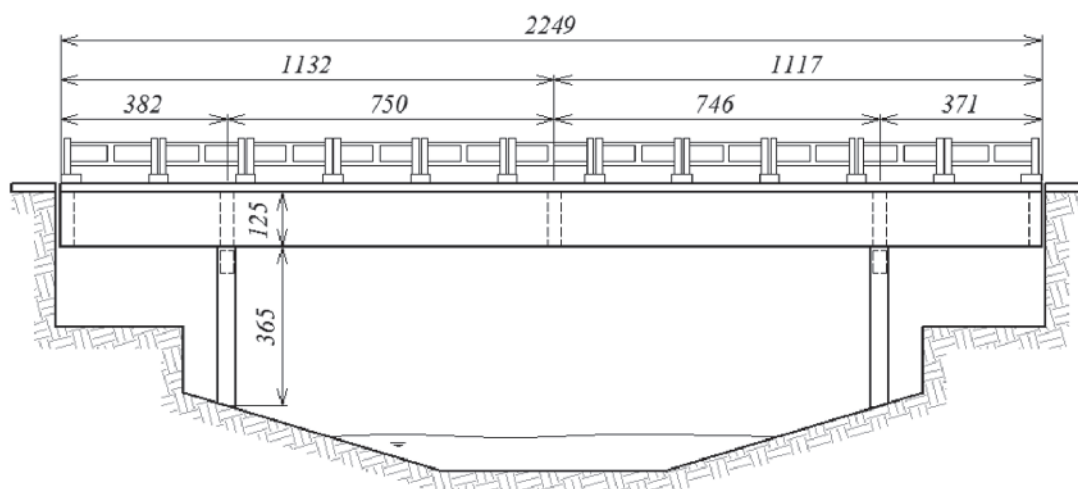


Figure 6
Lateral view of the Lambari bridge (dimensions in cm)

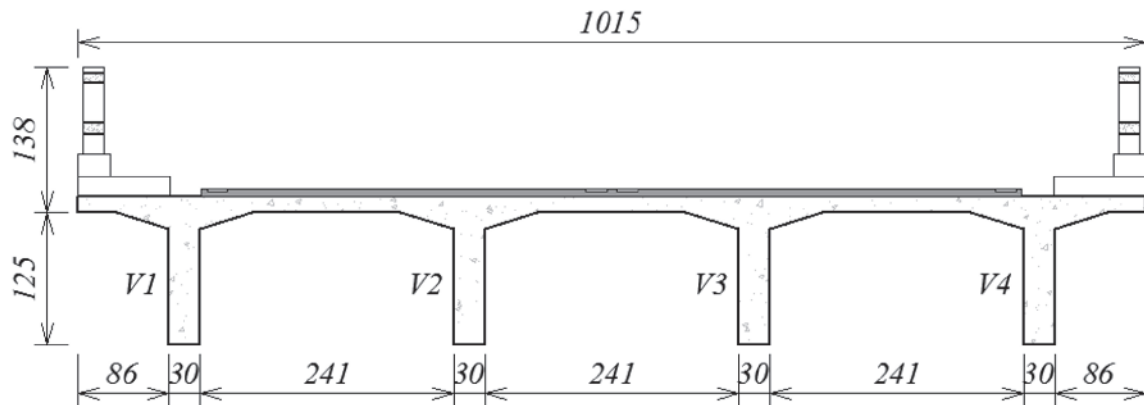


Figure 7
Superstructure cross section of the Lambari bridge (dimensions in cm)

to be Gaussian in the frequency domain [39]. This way the convolution process leads to better smoothed responses when compared to other filters. Figure 5 shows the bridge strain signal before and after the smoothing process.

2.4 Temperature effect

Differently from the transducers used in conventional weigh-in-motion systems installed in the pavement and directly exposed to the sun, the B-WIM systems' transducers are installed below the bridge superstructure, which leads to smaller temperature fluctuations over the day. In addition, the B-WIM system used in

the present study uses self-temperature-compensating transducers. Therefore, for small temperature variations, like the ones that usually occur below the superstructure, it is not expected that the measured strain values will be altered.

3. Case study: Lambari bridge

3.1 Bridge description

The object of the present study is a bridge over Lambari River, on BR-153 highway, km-153, municipality of Uruaçu (State of Goiás), Brazil. Figure 6 and Figure 7 show some geometry details of this

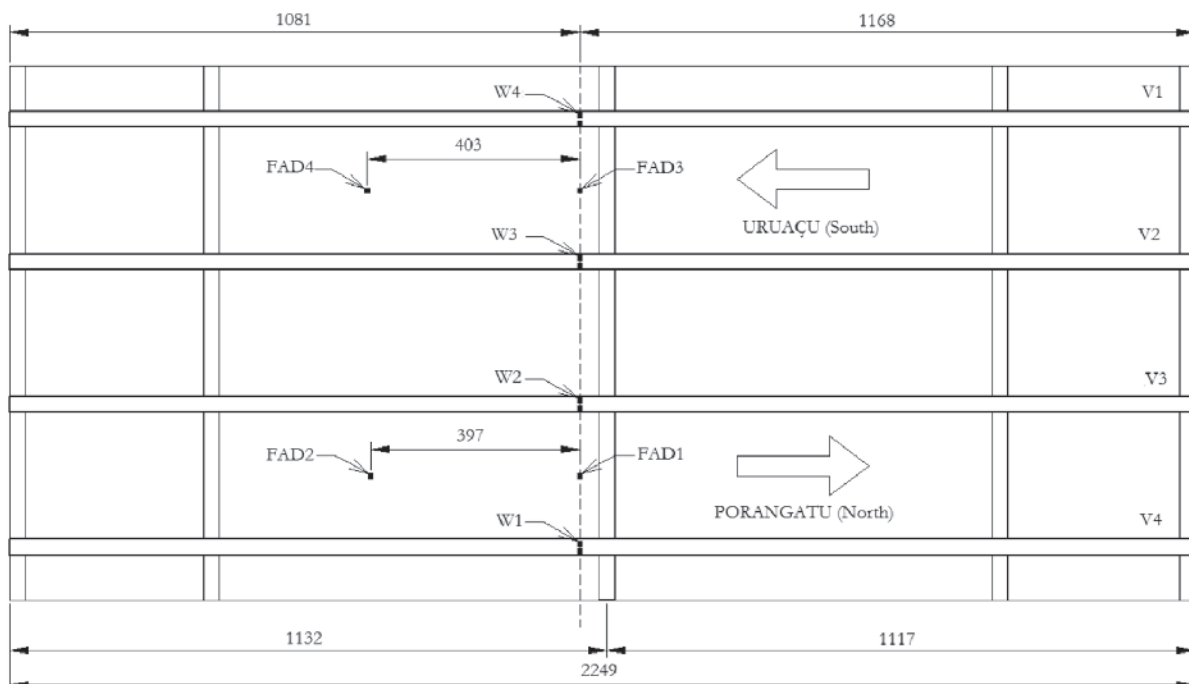


Figure 8
Transducers position on the superstructure

bridge. The structure is made of four main 15 m span girders supported by columns, with 3.75 m cantilevers at each edge, resulting in a total length of 22.5 m. Moreover, there are five cross beams: one at midspan, two above the columns and two at the edges.

This bridge was monitored by a B-WIM system between November of 2013 and January of 2014, for a total of 42 days, in order to assess its security level. Figure 8 shows the location of the transducers for weight measurement (W1, W2, W3 e W4) on the bottom face of the girders, near midspan, and also the FAD transducers (FAD 1, FAD 2, FAD 3 e FAD 4). FAD transducers were placed on the bottom face of the bridge deck in order to acquire more prominent peaks from the passage of a vehicle over the bridge.

3.2 System calibration

The B-WIM system was calibrated following COST 323 [8] report indications. Therefore, two trucks were used, one rigid with three axles and another semi-trailer with five axles. A total of 56 passages were performed for the two lanes, with 17 passages for lane 1 (South-North direction) and 19 passages for lane 2 (North-South direction). The trucks properties are shown in Table 1, with their weights indicated by static scale weighing.

Table 2 and Table 3 present the velocities and axles spacing obtained for the 17 passages on lane 1 and the 19 passages for lane

2, respectively, the errors of axles spacing for each passage when compared to the real values are also shown. It can be seen that the maximum absolute difference between the real spacing and the calculated one is 15 cm, which occurred in the second passage on lane 2, corresponding to a small error of just 3.25%. For the closed spaced axles, the highest errors are 6.17% and 6.19%, for lanes 1 and 2 respectively. Although this percentage is relatively high, these errors correspond to only 8 cm of difference between the real axle space and the calculated one.

The next step was to filter the signal in order to obtain the actual IL and the weighing of the traffic vehicles. The structure fundamental frequency was acquired by performing a frequency domain analysis in the free vibration part of the signals obtained during the passage of the calibration trucks. The frequency domain response for each passage was attained from a Fast Fourier Transform (FFT), as can be seen in Figure 9. The value of 10 Hz can be assigned as the structure fundamental frequency.

The complete signals of each calibration event in the frequency domain are presented in Figura 10, where one can verify that frequencies up to 2.5 Hz are responsible for great part of the amplitude in the structure response. Thus, this value was defined as the cut off frequency for the signal filtering. All passages signals were then filtered in frequency domain previously to the weighing process.

Table 1

Properties of the trucks used during the calibration process

Vehicle	Axles weights (kN)						Spacing between axles (m)			
	GVW	P1	P2	P3	P4	P5	d1-d2	d2-d3	d3-d4	d4-d5
Rigid (3 axles)	264.00	46.70	108.65	108.65	-	-	4.60	1.29	-	-
Semi-trailer (5 axles)	368.00	51.80	53.49	87.56	87.56	87.56	4.27	3.47	1.23	1.23

Table 2

Velocities and axles spacings obtained with FAD sensors for lane 1

Passage	Number of axles	Velocity (m/s)	Calculated axles spacings (m)				Error (%)			
			d1-d2	d2-d3	d3-d4	d4-d5	d1-d2	d2-d3	d3-d4	d4-d5
1	3	22.34	4.67	1.31	-	-	-1.48	-1.47	-	-
2	3	25.41	4.66	1.24	-	-	-1.41	3.82	-	-
3	3	25.73	4.67	1.26	-	-	-1.60	2.61	-	-
4	3	26.06	4.63	1.27	-	-	-0.69	1.36	-	-
5	3	22.84	4.59	1.29	-	-	0.12	-0.28	-	-
6	3	23.64	4.66	1.29	-	-	-1.36	-0.18	-	-
7	3	24.79	4.65	1.21	-	-	-1.04	6.17	-	-
8	3	24.20	4.63	1.23	-	-	-0.69	4.75	-	-
9	3	23.64	4.66	1.29	-	-	-1.36	-0.20	-	-
10	3	25.09	4.66	1.23	-	-	-1.22	5.01	-	-
11	3	18.15	4.64	1.24	-	-	-0.95	3.83	-	-
12	3	18.15	4.64	1.28	-	-	-0.95	1.08	-	-
13	5	21.62	4.27	3.51	1.27	1.27	0.10	-1.02	-3.00	-3.00
14	5	23.91	4.20	3.50	1.21	1.21	1.56	-0.95	1.27	1.27
15	5	23.91	4.30	3.46	1.26	1.21	-0.63	0.40	-2.54	1.27
16	5	24.79	4.21	3.53	1.21	1.26	1.36	-1.85	1.59	-2.34
17	5	23.64	4.20	3.55	1.20	1.25	1.62	-2.44	2.42	-1.32

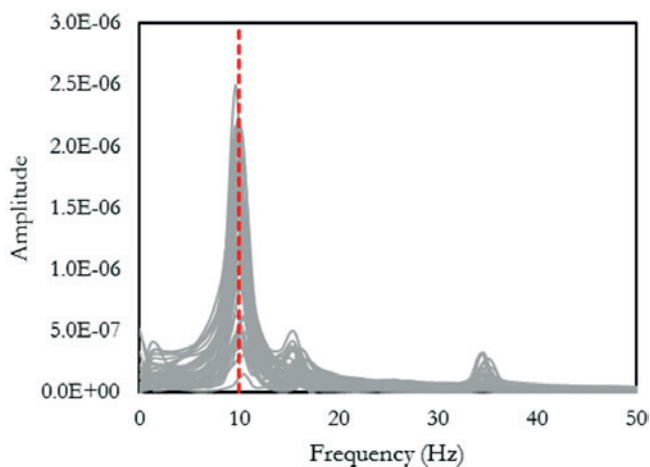


Figure 9
Fundamental frequency of the structure obtained experimentally

With the filtered data, it was attained the IL for lane 1 and lane 2, as shown on Figure 11, together with the theoretical IL. By observing this figure, three aspects can be highlighted: (i) calibration ILs present peaks inferior to the theoretical IL; (ii) calibration ILs are bigger in extension than the theoretical one and; (iii) lane 1 IL present an unexpected behavior, specifically near the South support. Related to the first aspect, it is clear that the real support conditions are different from the idealized theoretical ones, occurring a smoothing in the IL maximum value. The extension of the calibration ILs (second aspect) will always

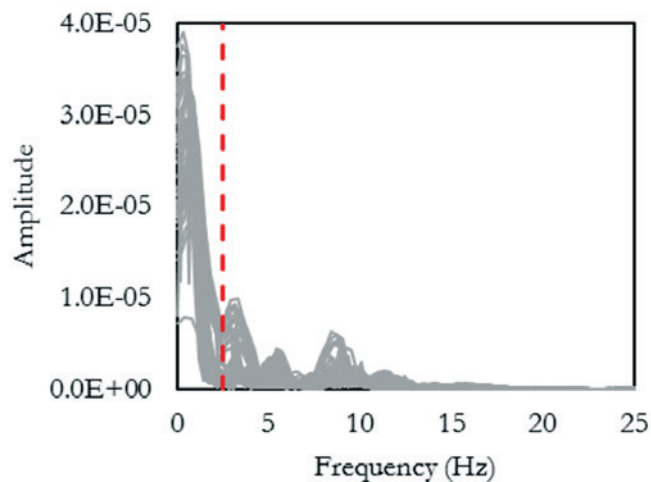


Figure 10
Response of the structure in the frequency domain

be bigger than the bridge length, because the readings start on the instant in which the vehicle enters the bridge (Figure 01) and do not end right after it leaves. In the application of Moses' method, when the first axle enters the bridge ($t = 0$), the other axles do not cause deformation, but they need to be taken into account. Furthermore, because the load is dynamic, the effects caused by the passage of the vehicle do not cease after its exit from the structure. In fact, the structure still presents free vibration response for a while. When this signal stretch is not considered, higher errors occur. Thus, it was decided to extend the IL

Table 3

Velocities and axles spacings obtained with FAD sensors for lane 2

Passage	Number of axles	Velocity (m/s)	Calculated axles spacings (m)				Error (%)			
			d1-d2	d2-d3			d1-d2	d2-d3		
1	3	24.56	4.70	1.25	-	-	-2.21	3.31	-	-
2	3	24.56	4.75	1.30	-	-	-3.25	-0.43	-	-
3	3	23.99	4.73	1.31	-	-	-2.89	-1.70	-	-
4	3	23.72	4.72	1.30	-	-	-2.71	-0.55	-	-
5	3	24.27	4.69	1.33	-	-	-2.04	-2.91	-	-
6	3	24.27	4.69	1.33	-	-	-2.04	-2.91	-	-
7	3	24.86	4.71	1.31	-	-	-2.38	-1.64	-	-
8	3	24.56	4.75	1.30	-	-	-3.25	-0.43	-	-
9	3	24.56	4.70	1.30	-	-	-2.21	-0.41	-	-
10	3	24.27	4.69	1.28	-	-	-2.04	0.76	-	-
11	3	18.76	4.73	1.28	-	-	-2.74	0.60	-	-
12	3	23.45	4.72	1.33	-	-	-2.54	-2.97	-	-
13	5	25.79	4.28	3.53	1.26	1.26	-0.28	-1.62	-2.39	-2.37
14	5	24.86	4.27	3.54	1.26	1.26	-0.07	-2.14	-2.65	-2.63
15	5	25.79	4.28	3.58	1.26	1.26	-0.28	-3.07	-2.39	-2.39
16	5	15.51	4.27	3.51	1.24	1.24	-0.06	-1.29	-1.00	-1.00
17	5	24.86	4.32	3.54	1.26	1.21	-1.20	-2.15	-2.63	1.31
18	5	21.72	4.33	3.52	1.31	1.23	-1.33	-1.47	-6.90	-0.02
19	5	17.05	4.26	3.53	1.27	1.23	0.16	-1.74	-2.90	-0.19

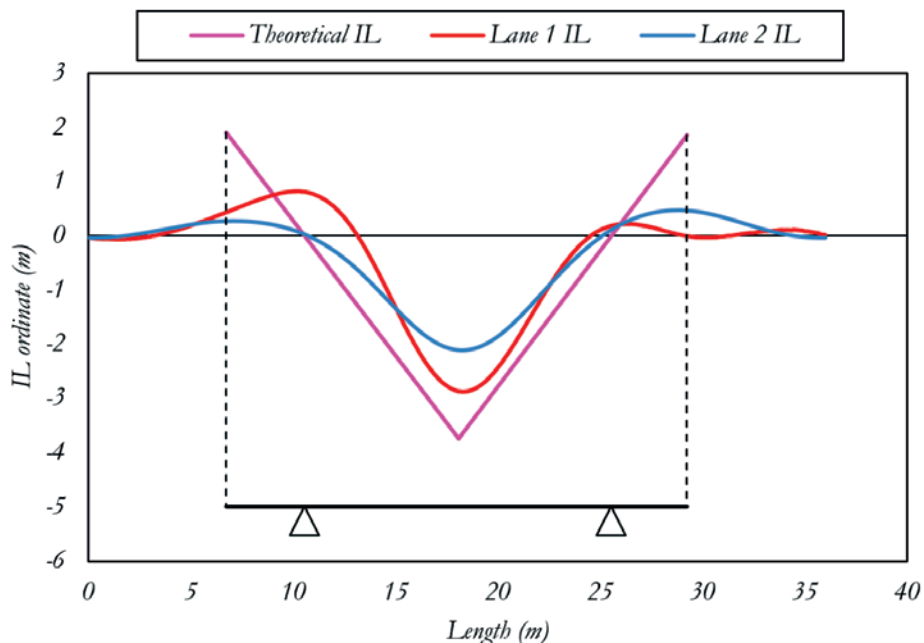


Figure 11
Comparison between ILs acquired during the B-WIM system calibration and the theoretical one

length beyond the bridge ends. It was observed that this extension directly influences the precision of the acquired weights. The extension must be adjusted case by case. For the bridge here analyzed, it was found the value of 36 m for the total extension as the one leading to lower relative errors. The characteristics of the IL of lane 1, both in terms of shape and

maximum value, have occurred due the large oscillation present in the signals originated by the presence of defects in the South entrance of the bridge. In this case, the filtering process was not effective to minimize the dynamic effects.

Using the obtained ILs, the axles weights and GVW of the calibration vehicles were calculated as described on item 2. Table 4

Table 4
Errors (%) acquired for the passages of the calibration vehicles on lane 1

Passage	P1	P2	P3	P4	P5	GVW
1	-5.65	-12.91	11.61	-	-	-1.53
2	-43.59	147.09	-126.97	-	-	0.57
3	-51.18	162.49	-142.75	-	-	-0.93
4	-47.67	128.14	-114.96	-	-	-3.01
5	-28.02	32.26	-26.39	-	-	-2.54
6	-23.10	61.20	-62.53	-	-	-4.63
7	-34.92	119.64	-110.40	-	-	-2.37
8	-21.15	90.92	-85.44	-	-	-1.48
9	-15.05	49.23	-51.42	-	-	-3.56
10	-33.40	109.00	-94.78	-	-	-0.06
11	-70.71	-5.24	56.76	-	-	8.70
12	-73.72	1.24	50.42	-	-	8.22
13	-43.31	80.15	-684.41	954.71	-324.55	2.75
14	11.14	-0.04	-79.57	30.72	42.71	0.08
15	-27.23	48.09	-241.83	188.07	15.18	0.22
16	-14.17	27.09	-54.20	-66.16	87.91	-1.98
17	2.12	13.72	-167.98	146.13	15.57	2.29
Absolute medium error	32.13	64.03	127.20	81.52	28,58	2.64

Table 5
Errors (%) acquired for the passages of the calibration vehicles on lane 2

Passage	P1	P2	P3	P4	P5	GVW
1	-1.42	12.02	-9.57	-	-	0.76
2	-3.07	6.45	-7.66	-	-	-1.04
3	12.02	-18.53	14.32	-	-	0.39
4	6.04	-16.34	14.34	-	-	0.25
5	14.17	-7.64	4.20	-	-	1.09
6	10.16	-4.44	2.41	-	-	0.96
7	-3.52	9.38	-7.47	-	-	0.16
8	5.00	2.71	-4.64	-	-	0.09
9	2.25	-1.95	2.25	-	-	0.52
10	2.60	9.51	-7.02	-	-	1.48
11	-0.64	-9.99	14.14	-	-	1.60
12	-2.64	-14.74	14.91	-	-	-0.40
13	-9.07	12.88	-86.10	116.08	-50.66	-2.34
14	0.13	9.07	-108.78	150.44	-58.35	-1.28
15	-6.12	16.98	-118.92	153.52	-62.74	-2.54
16	23.14	-42.22	237.69	-354.22	166.61	3.12
17	24.20	-15.29	-89.10	198.10	-105.49	0.02
18	13.20	-10.95	-31.11	71.07	-35.29	-0.05
19	27.47	-55.37	284.48	-388.59	167.11	3.17
Absolute medium error	8.78	14.55	55.74	75.37	34.01	1.11

and Table 5 bring the errors for axles weights and GVW for each passage during the calibration process when compared to the data in Table 1. Although the calibration vehicles had significantly different GVWs, the errors were compared together because the system must be robust in order to weigh vehicles with different characteristics with a certain confidence margin. As can be seen, the errors for individual axles weight are high, especially for the closed spaced ones. On the other hand, in relation to GVW, the errors are smaller, with maximum error of 8.70% for lane 1 and 3.17% for lane 2, and relative medium error inferior of 3% for both cases.

3.3 Traffic characterization

Figure 12 illustrates the vehicles histogram, based on number of axles, that crossed over Lambari bridge during the 42 days of monitoring. Vehicles up to three axles summed 52% of total traffic. The GVW of those vehicles, as expected, did not show high values as can be seen in the GVW histogram shown in Figure 13. For this histogram, it is also possible to observe that GVW superior to 300 kN were given by trucks with 6-axle and above which were responsible for the upper tail of the distribution.

The histograms of maximum bending moment at midspan are

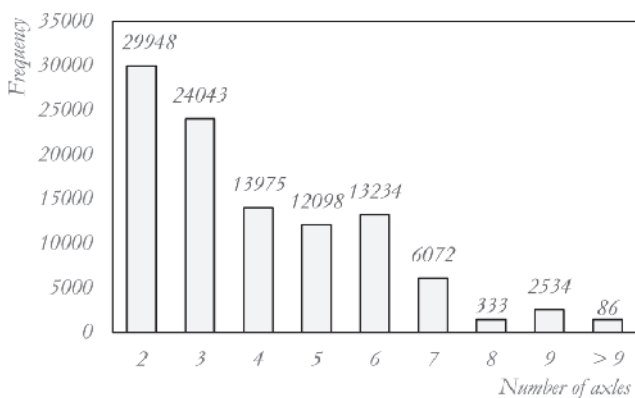


Figure 12
Vehicles histogram, based on number of axles, that traveled over Lambari bridge

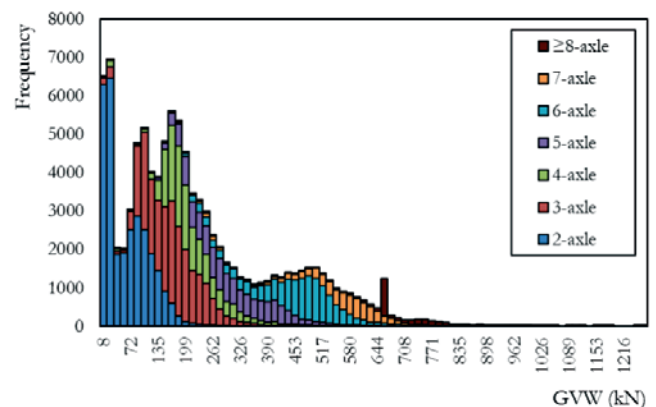


Figure 13
GVW histogram of the monitored vehicles

presented in Figure 14 for each girder. The histograms for girders V3 and V4 show higher dispersion of results when compared to the ones for girders V1 and V2. This happened due to the defects in the South entrance, leading the vehicles to generate more impact when entering the bridge, as can be observed also in lane 1 IL. The central girders, V2 and V3, were the most loaded ones, showing that traffic flowed close to the longitudinal axis of the bridge. For these girders, Figure 15 shows the bending moment histogram for each vehicle with more than 3 axles. As can be seen, vehicles with 3, 4 and 5 axles contributed significantly to the upper tail of the distribution, presenting maximum bending moments in the same magnitude as the ones introduced by vehicles with 6 or more axles. Figure 16 presents the dynamic amplification factor for each vehicle that traveled over the bridge during the 42 days of monitoring. It is observed that trucks with lower GVW present higher impact coefficient values, identifying an inversely proportional relationship between GVW and DAF. This behavior is in agreement with what was observed by [38]. Fitting a Fréchet distribution to the

measured cumulative probability distribution, as shown in Figure 16 (b), a value of 1.31 for DAF is obtained. This value is in agreement with the one indicated in the Brazilian Code NBR 7188 [40] for the analyzed bridge (1.33).

4. Conclusions

In the present study, results of the monitoring of a reinforced concrete bridge in Goiás State by means of a B-WIM system are presented. From these data, it can be concluded about the application of such system:

- The adopted procedure to acquire the Influence Line, implemented in the B-WIM system [31], has made possible to obtain the actual IL of the structure, representing the real support conditions.
- The FAD system for vehicle classification proved to be efficient in detecting the axles of the vehicles traveling alone on the bridge. However, when there is multiple presence this procedure is not recommended. If there is a need for accurate

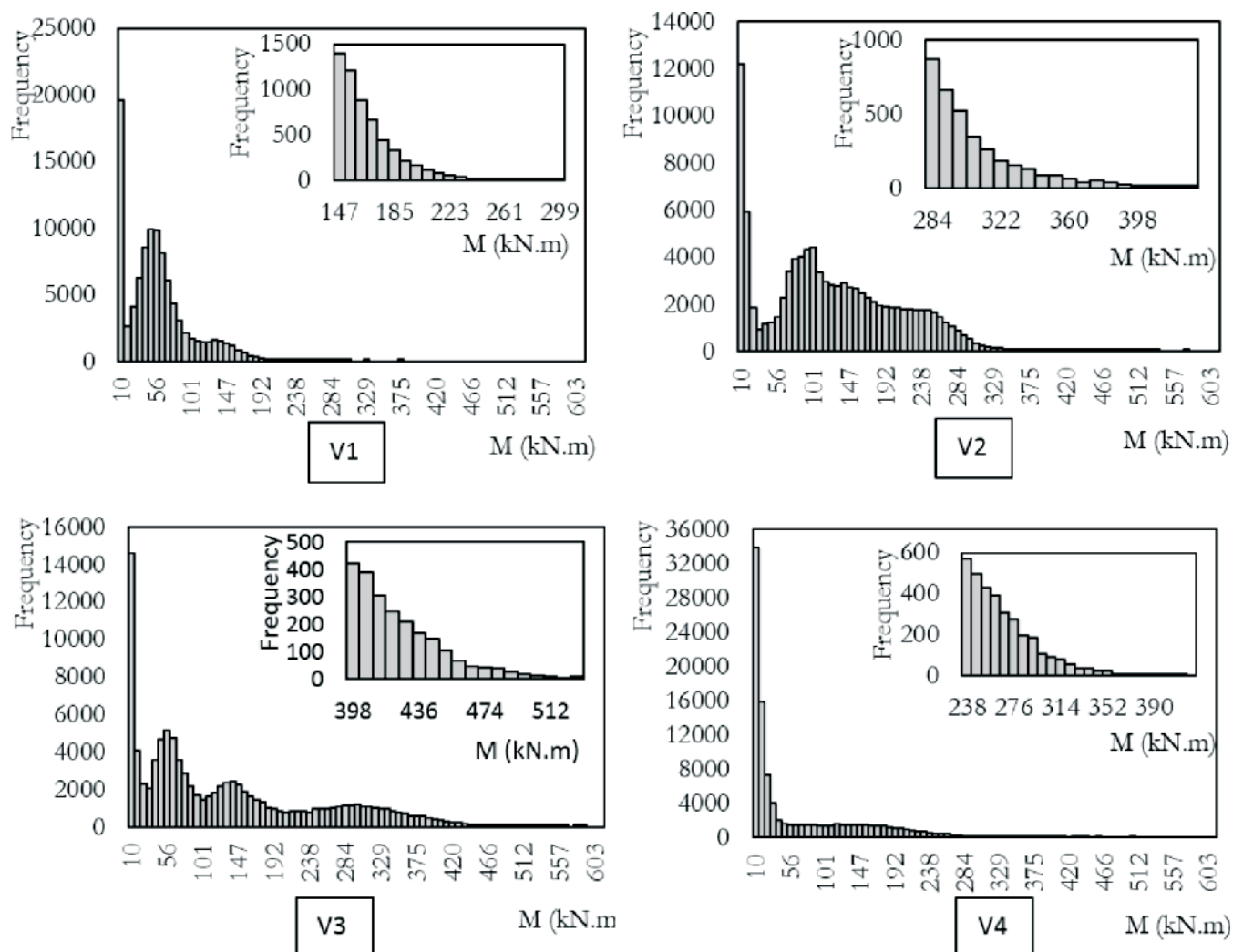


Figure 14
Bending moment histogram for each girder for the trucks passages during monitoring

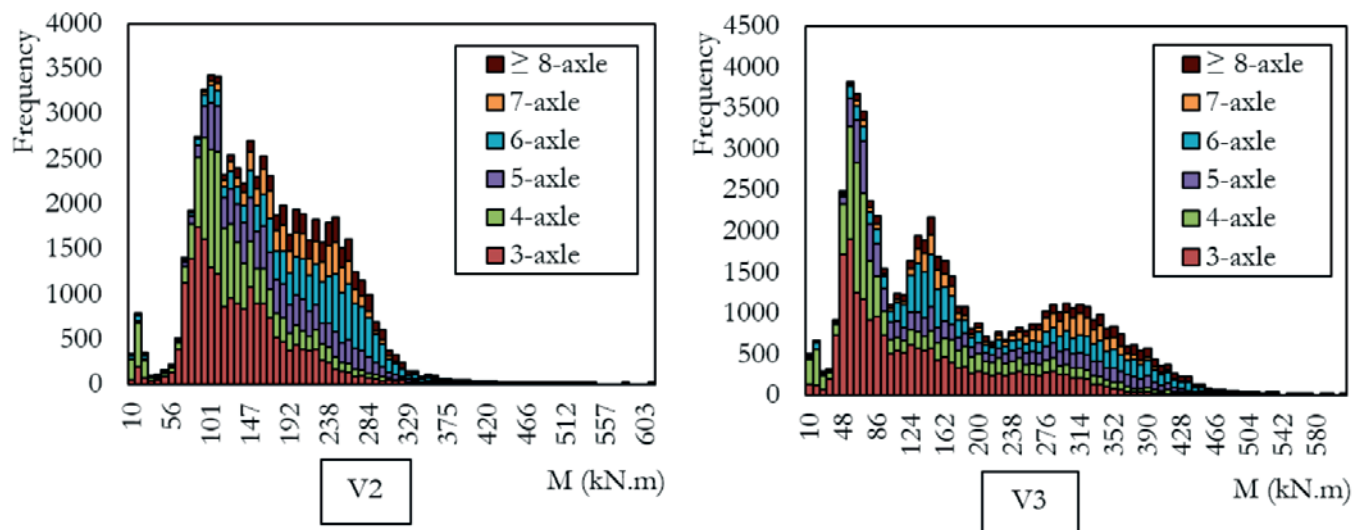


Figure 15
Bending moments histogram for girders V2 and V3 by means of vehicle class

classification of vehicles, image data must be used, so a 3-axle vehicle, e.g., can be classified either as a bus or a truck.

- The system provided good estimation of GVW. On the other hand, weight of isolated axles showed great variability. As a result, this study provided an indication that for the bridge analyzed, and the B-WIM system employed, only the traffic composition (silhouettes and velocities) and the GVW of vehicles could be adequately obtained.

From the monitoring data, it was possible to characterize the active

traffic in the logistic corridor studied and its impact on the bridge internal forces. From this analysis, the following conclusions are drawn:

- Vehicles with up to three axles made up more than half of the traffic during the period of monitoring.
- The vehicles tended to travel next to the longitudinal axis of the bridge instead of on rolling lanes, inducing greater stresses in the central girders.
- Even vehicles with relatively low GVW have introduced high stresses due to their higher dynamic amplification factor.

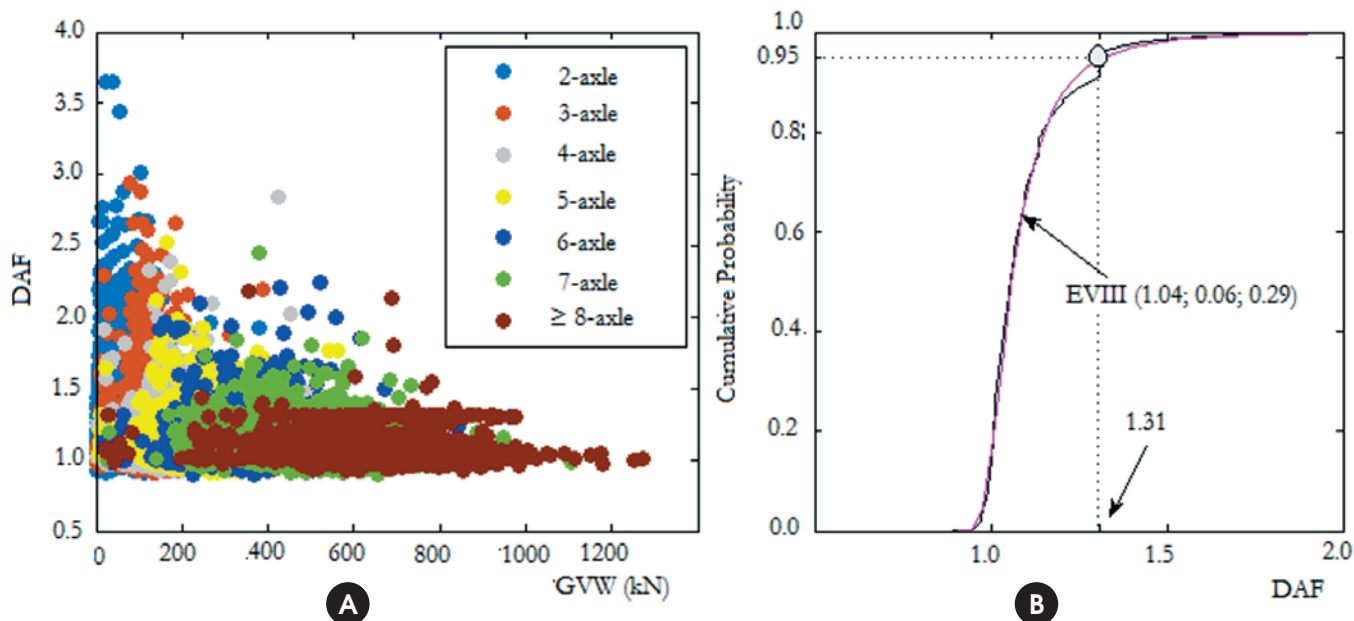


Figure 16
(a) Dynamic amplification factor (DAF) by vehicle type and (b) fitting a Fréchet function to the cumulative probability of DAF

5. Acknowledgements

The authors would like to thank the Transport Infrastructure National Department (DNIT) for the financial support and to the Foundation of Research Support and University Extension (FAPEU) and to the Foundation for Socioeconomic Studies (FEPESE) for the scholarships.

6. References

- [1] ASSOCIAÇÃO BRASILEIRA DE NORMAS TÉCNICAS. Cargas móveis em pontes rodoviárias. NB-6, Rio de Janeiro, 1960.
- [2] Žnidarič A. Kreslin M. Lavrič I. Kalin J. Simplified approach to modelling traffic loads on bridges. *Procedia – Social and Behavioral Sciences*, v.48, 2012, p.2887-2896.
- [3] O'Brien E. Žnidarič A. Ojio T. Bridge Weigh-in-Motion – latest developments and applications world wide. In: International Conference of Weigh-in-Motion, 5th, Paris, 2008, p.25-38.
- [4] Moses F. Weigh-in-Motion system using instrumented bridges. *ASCE Transp Eng J*, v.105, n.3, 1979, p.233-249.
- [5] Peters RJ. AXWAY - A system to obtain vehicle axle weights. In: Conference of the Australian Road Research Board, 12th, Hobart, 1984, p.19-29.
- [6] Peters RJ. CULWAY - an unmanned and undetectable highway speed vehicle weighing system. In Conference of the Australian Road Research Board, 13th, Adelaide, 1986, p.70-83.
- [7] O'Brien EJ. Žnidarič A. Weigh-in-Motion of Axles and Vehicles for Europe (WAVE). Report of Work Package 1.2: Bridge WIM systems (B-WIM), 2001, 100 p.
- [8] COST 323–Weigh-in-Motion of Road Vehicles - Final Report. Appendix 1: European WIM Specification, 1999.
- [9] Jacob B. Weigh-in-motion of Axles and Vehicles for Europe (WAVE) - General Report. 4th Framework Programme Transport. RTD project, RO-96-SC, 403, 2001.
- [10] Yamada K. Ojio T. Bridge weigh-in-motion system using reaction force method. In: International Workshop on Structural Health Monitoring of Bridges/Colloquium on Bridge Vibration, Japan Society of Civil Engineers, 2003, p.269-276.
- [11] Yu Y. Cai C. Deng L. State-of-the-art review on bridge weigh-in-motion technology. *Advances in Structural Engineering*, v.19, n.9, 2016, p.1514-1530.
- [12] Jiang RJ. Au FTK. Cheung YK. Identification of vehicles moving on continuous bridges with rough surface. *Journal of Sound and Vibration*, v.274, 2004, p.1045-1063.
- [13] Au FTK. Jiang RJ. Cheung YK. Parameter identification of vehicles moving on continuous bridges. *Journal of Sound and Vibration*, v.269, 2004, p.91-111.
- [14] Law SS. Bu JQ. Zhu XQ. Chan SL. Vehicle Condition Surveillance on Continuous Bridges Based on Response Sensitivity. *Journal of Engineering Mechanics*, v.132, n.1, 2006, p.78-86.
- [15] Deng L. Cai CS. Identification of parameters of vehicles moving on bridges. *Engineering Structures*, v.31, n.10, 2009, p.1514-1530.
- [16] Pan C. Yu L. Moving force identification based on firefly algorithm. *Advanced Materials Research*, v. 919, n.1, 2014, p.329-333.
- [17] Kim S. Lee J. Park M. Jo B. Vehicle Signal Analysis Using Artificial Neural Networks for a Bridge Weigh-in-Motion System. *Sensors*, v.9, 2009, p.7943-7956.
- [18] Leming SK. Stalford HL. Bridge weigh-in-motion system development using superposition of dynamic truck/static bridge interaction. In: American Control Conference, Denver, 2003.
- [19] Law SS. Bu JQ. Zhu XQ. Chan SL. Vehicle axle loads identification using finite element method. *Engineering Structures*, v.26, 2004, p.1143-1153.
- [20] González A. Rowley C. O'Brien EJ. A general solution to the identification of moving vehicle forces on a bridge. *Int. J. Numer. Meth. Engng*, v.75, 2008, p.335-354.
- [21] Rowley CW. O'Brien EJ. González A. Žnidarič A. Experimental Testing of a Moving Force Identification Bridge Weigh-in-Motion Algorithm. *Experimental Mechanics*, v. 49, 2009, p.743-746.
- [22] Deesomsuk T. Pinkaew T. Effectiveness of Vehicle Weight Estimation from Bridge Weigh-in-Motion. *Advances in Civil Engineering*, 2009, p.1-13.
- [23] Karoumi R. Wiberg J. Liljencrantz A. Monitoring traffic loads and dynamic effects using an instrumented railway bridge. *Engineering Structures*, v.27, n.12, 2005, p.1813-1819.
- [24] Carvalho Neto JA. Veloso LACM. Weighing in motion and characterization of the railroad traffic with using the B-WIM technique. *Ibracon Structures and Materials Journal*, v.8, n.4, 2015, p.491-506.
- [25] Žnidarič J. Žnidarič A. Evaluation of the carrying capacity of existing bridges – Final Report. Institute for Testing and Research in Materials and Structures, Ljubljana, 1994.
- [26] Žnidarič A. Baumgartner W. Bridge Weigh-in-Motion systems – an overview. In: European Conference of Weigh-in-Motion of Road Vehicles, 2nd, Lisbon, 1998, p.139-152.
- [27] McNulty P. Testing of an Irish Bridge Weigh-in-Motion System, Dublin, 1999, Thesis (Master) - University College Dublin.
- [28] González A. O'Brien EJ. Influence of Dynamics on Accuracy of a Bridge Weigh-in-Motion System. In: Conference of Weigh-in-Motion, 3rd, Orlando, 2002.
- [29] McNulty P. O'Brien EJ. Testing of Bridge Weigh-in-Motion System in a Sub-Arctic Climate. *Journal of Testing and Evaluation*, v.31, n.6, 2003.
- [30] Quilligan M. Bridge Weigh-in-Motion: Development of a 2-D Multi-Vehicle Algorithm, Stockholm, 2003, Thesis (Phd) - Structural Design and Bridge Division, Royal Institute of Technology, 160 p.
- [31] O'Brien EJ. Quilligan M. Karoumi R. Calculating an influence line from direct measurements. In: ICE Bridge Engineering, v.159, n.1, 2005, p.31-34.
- [32] Junges P. Pinto RCA. Fadel Miguel LF. Linha de influência real de pontes utilizando sistemas BWIM. In: Congresso Brasileiro do Concreto, 56^o, Anais, Natal, 2014.
- [33] Ieng S. Bridge influence line estimation for Bridge Weigh-in-Motion System. *Journal of Computing in Civil Engineering*, v.29, 2015.

- [34] Heinen S. Pinto RCA. Fadel Miguel LF. Junges P. Effect of transverse load distribution on the influence lines given by a bridge weigh in motion system. In: International Conference on Bridge Maintenance, Safety and Management, 8th, Anais, Foz do Iguaçu, 2016.
- [35] Žnidarič A. Žnidarič J. Terčelj S. Determination of the true traffic load in the process of safety assessment of existing bridges. In: Congress of Structural Engineers of Slovenia, 12th, Anais, 1991, p.241-246.
- [36] ISWIM. Weigh-in-Motion of Road Vehicles, 2013.
- [37] Žnidarič A. Lavrič I. Kalin J. The next generation of bridge weigh-in-motion systems. In: International Conference of Weigh-in-Motion, 3rd, 2002.
- [38] ARCHES. Deliverable D10: Recommendations on dynamic amplification allowance, (2009).
- [39] Gonzalez RC. Woods RE. Digital image processing. Pearson, 3ed, 2007, 976 p.
- [40] ASSOCIAÇÃO BRASILEIRA DE NORMAS TÉCNICAS. Carga móvel rodoviária e de pedestres em pontes, viadutos, passarelas e outras estruturas. NBR 7188, Rio de Janeiro, 2013.